DMD Fast Forward. Published on October 24, 2006 as doi:10.1124/dmd.106.011932
This article has not been copyedited and formatted. The final version may differ from this version.

DMD 011932

INVOLVEMENT OF MULTIPLE CYTOCHROME P450 AND UDP-GLUCURONOSYLTRANSFERASE ENZYMES IN THE IN VITRO METABOLISM OF MURAGLITAZAR

Donglu Zhang, Lifei Wang, Gamini Chandrasena, Li Ma, Mingshe Zhu, Hongjian Zhang, Carl D Davis, and W Griffith Humphreys

Pharmaceutical Candidate Optimization, Pharmaceutical Research Institute, Bristol-Myers Squibb, Princeton, NJ 08543

DMD Fast Forward. Published on October 24, 2006 as DOI: 10.1124/dmd.106.011932
This article has not been copyedited and formatted. The final version may differ from this version.

DMD 011932

Running title: Reaction-phenotyping for metabolism of muraglitazar

Address correspondence to:
Donglu Zhang, Ph.D.
Pharmaceutical Candidate Optimization,
Bristol-Myers Squibb, P.O. BOX 4000,
Princeton, NJ 08543.
Phone: 609-252-5582.
Email: Donglu.Zhang@BMS.com

[1]Abbreviations used: HLM, human liver microsomes; LC/MS, liquid chromatography/mass spectrometry; NADPH, β-nicotinamide adenine dinucleotide phosphate sodium (reduced form); PPAR, peroxisome proliferator-activated receptors; UDPGA, uridine 5'-diphospho-glucuronic acid; UGT, uridine 5'-diphospho-glucuronosyltransferase; TFA, trifluoroacetic acid

Text pages including references: 29

# of tables: 7; # of figures: 8

# of references: 28

# of words in abstract: 245

# of words in introduction: 500

# of words in discussion: 1200

ABSTRACT

Muraglitazar (Pargluva), a dual alpha/gamma peroxisome proliferator-activated receptor activator, has both glucose and lipid lowering effects in animal models and in patients with diabetes. The human major primary metabolic pathways of muraglitazar include acylglucuronidation, aliphatic/aryl hydroxylation, and *O*-demethylation. This study describes the identification of human CYP and UGT enzymes involved in the *in vitro* metabolism of muraglitazar. [^{14}C]Muraglitazar was metabolized by cDNA expressed CYP2C8, 2C9, 2C19, 2D6, and 3A4, but to a very minimal extent by CYP1A2, 2A6, 2B6, 2C18, 2E1, and 3A5. Inhibition of the in vitro metabolism of muraglitazar in human liver microsomes, at a clinically efficacious concentration, by chemical inhibitors and monoclonal antibodies further supported involvement of CYP2C8, 2C9, 2C19, 2D6, and 3A4 in its oxidation. A combination of intrinsic clearance (V_{max}/K_m) and relative concentrations of each CYP enzyme in the human liver was used to predict the contribution of CYP2C8, 2C9, 2C19, 2D6, and 3A4 to the formation of each primary oxidative metabolite and to the overall oxidative metabolism of muraglitazar. Glucuronidation of [^{14}C]muraglitazar was catalyzed by cDNA expressed UGT1A1, 1A3, and 1A9, but not by UGT1A6, 1A8, 1A10, 2B4, 2B7, and 2B15. The K_m values for muraglitazar glucuronidation by the three active UGT enzymes were similar (2-4 μM). In summary, muraglitazar was metabolized by multiple CYP and UGT enzymes to form multiple metabolites. This characteristic predicts a low potential for the alteration of the pharmacokinetic parameters of muraglitazar via polymorphic drug metabolism enzymes responsible for clearance of the compound or by co-administration of drugs that inhibit or induce relevant metabolic enzymes.

INTRODUCTION

Cytochrome P450 (CYP, EC1.14.14.1) enzymes play a key role in the clearance of many drugs and alteration of the activity of these enzymes is the major cause of drug-drug interactions. CYP enzymes comprise a super-family of hemoproteins residing on the cytoplasmic face of the endoplasmic reticulum membranes. Together with cytochrome P450 reductase, CYP enzymes catalyze a variety of types of oxidation reactions such as hydroxylation and dealkylation (Nelson et al., 1996). Three families of CYP enzymes (CYP1, CYP2, and CYP3) are involved in the metabolism of most of xenobiotics in humans, with CYP1A2, 2A6, 2B6, 2C8, 2C9, 2C19, 2D6, and 3A4/5 are responsible for the metabolism of the majority of drugs. Glucuronidation represents a major biotransformation pathway that increases the elimination of many lipophilic drugs and /or metabolites. UDP-glucuronosyltransferases (UGTs) are a super-family of enzymes that use UDPGA as a cofactor and reside on the lumen side of the endoplasmic reticulum membranes (Miners and Mackenzie, 1991). There are two subfamilies of UDP-glucuronosyltransferases involved in drug metabolism in humans, UGT1A and UGT2B (Wells et al., 2004). A total of 18 human UGT enzymes have been characterized to date (Wells et al., 2004). UGT enzymes catalyze glucuronidation reactions at nucleophilic functional group such as a hydroxyl, carboxylic acid, or amine leading to the formation of β-D-glucuronic acid conjugates (King et al., 1996; Senafi et al., 1994).

Muraglitazar (Pargluva, BMS-298585), *N*-[(4-methoxyphenoxy)carbonyl]-*N*-[[4-[2-(5-methyl-2-phenyl-4-oxazolyl)ethoxy] phenyl]methyl]glycine), is an oxybenzyl-glycine analog (non-thiazolidinedione) and a novel dual alpha/gamma PPAR activator (Devasthale et al., 2005). Muraglitazar has both glucose and lipid lowering effects when

tested in animal models of diabetes and dyslipidemia and in patients with diabetes (Devasthale et al., 2005; Harrity et al., 2006; Kendall et al., 2006). Following oral administration to humans, [^{14}C]muraglitazar underwent extensive metabolism by both oxidation and glucuronidation pathways (Zhang et al., 2006; Wang et al., 2006). Fecal excretion was the major elimination pathway for [^{14}C]muraglitazar (>95% of the recovered dose) and metabolites including 12-hydroxy muraglitazar (M10), 17-hydroxy muraglitazar (M11), 9-hydroxy muraglitazar (M14), *O*-demethyl muraglitazar (M15), 12-hydroxy *O*-demethyl muraglitazar (M5) were the predominant drug-related components in the feces while formation of *O*-dealkyl muraglitazar (M1), and oxazole-ring opening metabolites (M9 and M16) were relatively minor metabolic pathways for muraglitazar (Zhang et al., 2006). The structures of these metabolites are shown in Figure 1. Human bile collected with an oral-gastro-duodenal tube during a limited collection period of 3-8 h post dose contained 40% of the dose-related material, 70% of which were glucuronide conjugates of muraglitazar and its oxidative metabolites. These results suggested that muraglitazar was cleared primarily by hepatic metabolism and excreted into the bile mainly as glucuronide conjugates (Wang et al., 2006).

The objective of this study was to identify the predominant human CYP and UGT enzymes responsible for the *in vitro* metabolism of muraglitazar. [^{14}C]Muraglitazar was incubated with human cDNA-expressed CYPs and UGTs to determine the catalytic turnover for oxidation and direct glucuronidation of muraglitazar. The individual enzymes involved in muraglitazar biotransformation were further investigated in studies with specific inhibitory antibodies and selective chemical CYP inhibitors in human liver microsomes. Kinetic parameters for metabolite formation were determined in incubations

with both human liver microsomes and cDNA expressed enzymes. The intrinsic clearance determined for each CYP enzyme, together with the relative concentration of each CYP enzyme in the human liver, was used to estimate the contribution of each enzyme to the formation of a particular metabolite and to the overall metabolism of muraglitazar. The results predict that multiple CYP and UGT enzymes will be involved in the metabolic clearance of muraglitazar.

MATERIALS AND METHODS

Materials. [^{14}C]Muraglitazar (specific radioactivity 8.4 μCi/mg, radiochemical purity 99.6%) was synthesized at Bristol-Myers Squibb. Its structure and the position of the radiolabel are shown in Figure 1. The synthesis and characterization of C-14 labeled muraglitazar will be published separately. Alamethicin, magnesium chloride, β-nicotinamide adenine dinucleotide phosphate (β-NADPH), and uridine diphosphoglucuronic acid (UDPGA) were obtained from Sigma-Aldrich Co. (St. Louis, MO). Sodium phosphate and trifluoroacetic acid (TFA) were obtained from EM Science (Gibbstown, NJ). Pooled human liver microsomes (HLM, prepared from 22 donors), membranes from insect cells transfected with baculovirus containing cDNA of human *CYP*s (CYP1A2, 2A6, 2B6, 2C8, 2C9, 2C18, 2C19, 2D6, 2E1, 3A4 and 3A5), and *UGT*s (UGT1A1, 1A3, 1A4, 1A6, 1A8, 1A9, 1A10, 2B4, 2B7, and 2B15), and CYP inhibitors (furafylline, 8-methoxypsoralen, orphenadrine, sulfaphenazole, tranylcypromine, quinidine, ketoconazole, montelukast, benzylnirvanol, 1-aminobenzotriazole) were purchased from Gentest, BD Biosciences Corporation (Woburn, MA). Two batches of pooled human liver microsomes, designated HLM A and HLM B, were used in this study. As indicated on the manufacturer's data sheet, HLM A contained 360, 320, and 570 pmol/mg of total P450, cytochrome CYP reductase, and cytochrome b5, respectively, and HLM B contained 240, 340, and 500 pmol/mg of total P450, cytochrome CYP reductase, and cytochrome b5, respectively. CYP enzyme activities with respect to the metabolism of specific probe substrates were also different: 240, 3100, 48, 71, 6800 pmol/min/mg proteins in HLM A versus 500, 1700, 26, 70, 4200 pmol/min/mg proteins in HLM B for CYP2C8, 2C9, 2C19, 2D6, and 3A4, respectively. Further characterization

of specific enzyme content was not carried out. Inhibitory monoclonal anti-human CYP antibodies for CYP1A2, 2A6, 2B6, 2C8, 2C9, 2C19, 2Cs, 2D6, 2E1, 3A4 were obtained from the National Institute of Health (NIH) (Gelboin and Krausz, 2006). Cryopreserved human hepatocytes from three donors were purchased from In Vitro Technologies (Baltimore, MD). Acetonitrile was purchased from Allied Signal Inc (Muskegow, MI). All other organic solvents and water were of HPLC grade. Stock solutions of 5.17 mM [^{14}C]muraglitazar were prepared by dissolving 2.67 mg [^{14}C]muraglitazar in 1 mL of water/acetonitrile (1:1, v/v). CYP inhibitor stock solutions (1-20 mM) were prepared in acetonitrile and all aliquots were kept at –20°C. NADPH and UDPGA stock solutions (10-12 mM) were prepared in water prior to use.

Incubations with human cDNA expressed CYPs and HLM in the presence of NADPH, and in human hepatocytes. [^{14}C]Muraglitazar was incubated with human cDNA expressed CYP enzymes (CYP1A2, 2A6, 2B6, 2C8, 2C9, 2C18, 2C19, 2D6, 2E1, 3A4, or 3A5) in duplicate. The reaction mixtures consisted of 200 pmol/mL of CYP enzyme or 1 mg/mL of human liver microsomes (pooled HLM A), 26.6 μM of [^{14}C]muraglitazar, 1 mM NADPH, and 0.1 M sodium phosphate buffer, pH 7.4. The final volume of the incubation mixture was 0.25 mL. After a 30 min incubation at 37^{o}C with shaking (100 RPM), 0.25 mL of ice-cold acetonitrile was added to each tube to stop the reaction. The samples were centrifuged for 10 min at 2000xg. After centrifugation, aliquots of 75 μL of supernatant were analyzed by HPLC.

For substrate concentration-dependent metabolite formation studies, [^{14}C]muraglitazar at seven substrate concentrations (0, 10, 15, 25, 40, 65, and 150 μM) was incubated for 20 min with 1 mg/mL HLM A or cDNA expressed CYP enzymes supplemented with 1

DMD Fast Forward. Published on October 24, 2006 as DOI: 10.1124/dmd.106.011932
This article has not been copyedited and formatted. The final version may differ from this version.

mg/mL of heat-inactivated HLM at 37°C. The incubation mixtures were prepared in the same way as described above. The amount of each CYP enzyme (CYP2C8, 2C9, 2C19, 2D6, or 3A4) was 40 pmol/mL in each incubation. Under these conditions, the amount of each metabolite formed was linear with the protein concentrations and the incubation time up to 35 min.

[^{14}C]Muraglitazar (25 μM) was incubated with 2 million cells/mL human hepatocytes in 2 mL of buffer for 3 hours at 37°C. Ice-cold acetonitrile (2 mL) was added to stop the reaction. The samples were centrifuged for 10 min at 2000xg. After centrifugation, aliquots of 100 μL of supernatant were analyzed by HPLC.

HLM incubations in the presence of chemical CYP inhibitors

Effects of CYP inhibitors on total muraglitazar metabolism as measured by disappearance of the parent. Chemical CYP inhibitors were incubated with HLM B and muraglitazar in triplicate. Each reaction mixture (0.2 mL) contained 10 μL of 1 M phosphate buffer to a final concentration of 50 mM, 145 μL water, 10 μL of 100 mM $MgCl_2$ to a final concentration of 5 mM, 5 μL HLM B to a final concentration of 0.5 mg/mL, and 2-5 μL inhibitors or water. The final pH was 7.4. The mixture was incubated at 37°C for 10 min before 5 μL of 0.0516 mg/mL muraglitazar to a final concentration of 2.5 μM and 20 μL of NADPH to a final concentration of 1.2 mM were added to initiate the reactions. Chemical inhibitors were montelukast for CYP2C8 (Walsky et al., 2005), sulfaphenazole for CYP2C9 (Newton et al., 1995; Mancy et al., 1996), benzylnirvanol for CYP2C19 (Suzuki et al., 2002), quinidine for CYP2D6, ketoconazole for CYP3A4, and 1-aminobenzotriazole as a general CYP enzyme inhibitor and the respective concentrations used were 3, 10, 1, 1, 1, and 1000 μM. At these specific

DMD Fast Forward. Published on October 24, 2006 as DOI: 10.1124/dmd.106.011932
This article has not been copyedited and formatted. The final version may differ from this version.

concentrations, the chemical inhibitors are specific to the corresponding enzymes. Although ketoconazole at a 1 μM concentration showed a better inhibition selectivity for *in vitro* experiments, the clinical C_{max} in human subjects was 5-15 μM following 200 mg twice a day or 400 mg once a day dose regimens (Huang et al., 1986). Some of these inhibitors at a higher concentration were also used to test their inhibition selectivity. After the incubation for 30 min at 37°C with shaking (100 RPM) in a water bath, 0.4 mL acetonitrile containing 3% of acetic acid and 1.5 μg/mL of an internal standard (MS/MS transition was m/z 531 to 292) was added to quench the reactions. The mechanism-based inhibitor, 1-aminobenzotriazole, was pre-incubated with microsomes in the presence of NADPH for 10 min before muraglitazar was added. After the samples were centrifuged for 15 min at 2000xg, the supernatants were diluted with acetonitrile/water (2:1, v/v) before analysis by LC/MS.

Effect of CYP inhibitors on formation of muraglitazar metabolites. Chemical CYP inhibitors were incubated with HLM A and [^{14}C]muraglitazar in duplicate. Each 1 mL of incubation mixture contained 100 μL of 1 M phosphate buffer, pH 7.4, 100 μL of NADPH (10 mM), 5 μL of selective inhibitors, 5 μL of [^{14}C]muraglitazar (5.17 mM), 50 μL of HLM (20 mg/mL), and 740 μL of water. Mechanism-based inhibitors, furafylline, orphenadrine, and 1-aminobenzotriazole, were pre-incubated with microsomes in the presence of NADPH for 10 min before the substrate was added. The volume of organic solvent (acetonitrile) in the incubations was kept to a minimum (<0.5%, v/v). Each of these samples was incubated for 15 min at 37°C while shaking (100 RPM). After the incubation, 1.5 mL of ice-cold acetonitrile was added to each tube to stop the reaction. After the samples were centrifuged for 15 min at 2000xg, the supernatants were dried

DMD Fast Forward. Published on October 24, 2006 as DOI: 10.1124/dmd.106.011932
This article has not been copyedited and formatted. The final version may differ from this version.

under N_2, and the residues were reconstituted in 300 μL water/acetonitrile (2:1, v/v). An aliquot of 75 μL each sample was analyzed by HPLC.

HLM B incubations in the presence of inhibitory antibodies. Antibodies were incubated with HLM B and muraglitazar in triplicate. A reaction mixture (0.2 mL) contained 10 μL of 1 M phosphate buffer to a final concentration of 50 mM (pH 7.4), 145 μL water, 10 μL of 100 mM $MgCl_2$ to a final concentration of 5 mM, 5 μL HLM B to a final concentration of 0.5 mg/mL, and 2-5 μL antibodies or water. The mixture was incubated at 37°C for 10 min before 5 μL of 0.0516 mg/mL muraglitazar was added to a final concentration of 2.5 μM, and 20 μL of NADPH to a final concentration of 1.2 mM were added to initiate the reactions. After the incubation for 30 min at 37°C with shaking (100 RPM) in a water bath, 0.4 mL acetonitrile containing 3% of acetic acid and 1.5 μg/mL of an internal standard (MS/MS transition was m/z 531 to m/z 292) was added to quench the reactions. After the samples were centrifuged for 15 min at 2000xg, the supernatants were diluted with 2:1 (v:v) acetonitrile/water before analysis by LC/MS.

Under similar conditions, [^{14}C]muraglitazar (25 μM) was incubated with HLM B in the presence of 3 μM montelukast, or 5 μL/mL anti-CYP2C8 antibody. After the samples were centrifuged for 15 min at 2000xg, the supernatants were analysis by HPLC with the effluent split 4:1 to a fraction collector for radioactivity determination in conjunction with LC/MS.

HLM A incubations with cDNA expressed UGTs in the presence of UDPGA. Incubation mixtures (total volume 0.5 mL) contained 25 mM tris(hydroxymethyl)-aminomethane HCl buffer (pH 7.5), 10 mM $MgCl_2$, 25 μg/mL alamethicin, HLM A (0.8 mg protein/mL) or UGT enzyme (UGT1A1, 1A3, 1A4, 1A6, 1A8, 1A9, 1A10, 2B4, 2B7,

DMD Fast Forward. Published on October 24, 2006 as DOI: 10.1124/dmd.106.011932
This article has not been copyedited and formatted. The final version may differ from this version.

and 2B15) at a protein concentration of 0.1 mg protein/mL, and 26.6 μM [^{14}C]muraglitazar. The mixtures were pre-incubated at 37^{o}C for 5 min, then UDPGA (2.5 mM) was added to start the reaction. After a 30 min incubation at 37^{o}C with shaking (100 RPM), 0.5 mL of ice-cold acetonitrile was added to stop the reaction. The samples were centrifuged for 15 min at 2000xg. After centrifugation, an aliquot of 100 or 200 μL supernatant was used for HPLC analysis.

For enzyme kinetic studies, HLM A or human cDNA expressed UGT enzymes (UGT1A1, UGT1A3, or UGT1A9) were incubated with [^{14}C]muraglitazar in triplicate. The concentrations of [^{14}C]muraglitazar were 0, 2, 4, 6, 8, 10, 15, 20, and 30 μM. The protein concentration was 0.1 mg/mL for each UGT enzyme or for HLM. The formation of [^{14}C]muraglitazar glucuronide was linear up to 40 min (for UGT1A1, UGT1A3, and UGT1A9) at a concentrations of 10 μM (UGT1A9) or 30 μM (UGT1A1 or UGT1A3) of [^{14}C]muraglitazar and up to 0.2 mg/mL of cDNA expressed UGT enzyme.

HPLC analysis. HPLC was performed on a Shimadzu Class VP® system equipped with two pumps (model LC-10AT), an auto-injector (SIL 10AD), and a diode array detector (SPD-M10A; Shimadzu, Kyoto, Japan). YMC ODS AQ C-18 4.6x150 mm columns (5 micron, Waters) were used for radioactivity profiling. The HPLC flow was 1 mL/min. HPLC effluent fractions were collected into 96-well Lumaplates® at 0.26 min intervals for 70 min after sample injection with a Gilson Model 202 fraction collector (Gilson Medical Electronics, Middleton, WI). The plates were dried in a Speed-Vac® (Savant Instruments, Holbrook, NY) and analyzed with a TopCount® analyzer (PerkinElmer Life and Analytical Sciences, Boston, MA). Two solvents, A and B, were used for HPLC elution. Solvent A was water containing 0.06% TFA. Solvent B was acetonitrile

containing 0.06% TFA. The gradient started with 5% Solvent B. The composition of B increased linearly to 25% (5 min), 40% (15 min), 53% (40 min), 60% (3 min), and 90% (2 min), and was then held at 90% for 7 min.

LC/MS/MS identification of muraglitazar metabolites. Mass spectral analysis was performed on a Finnigan LCQ XP mass spectrometer (ThermoFinnigan, San Jose, CA) with an ESI probe. Samples were analyzed in the positive ionization mode. A Waters YMC ODS-AQ™ S-3 µm 120 Å column (2.0 x 150 mm) was used for HPLC and a heater maintained column temperature at 35°C. The mobile phase flow rate was 0.31 mL/min. The HPLC effluent was directed to the mass spectrometer through a divert-valve set to divert the flow to waste from 0-5 min. The capillary temperature was set at 210°C. The nitrogen gas flow rate, spray current, and voltages were adjusted to give maximum sensitivity for muraglitazar.

LC/MS/MS quantification of muraglitazar in incubations with HLM B. The concentration of muraglitazar was determined by an LC/MS/MS method. After microsomal incubation mixtures were centrifuged for 5 min, 50 µL of supernatant was diluted with 950 µL acetonitrile/water (1:1) and 10 µL was injected onto the LC/MS/MS system. A Shimadzu pump system (Shimadzu Corp., Columbia, MD) integrated with CTC PAL autosampler (Carrboro, NC) and YMC ODS-AQ column (2 x 50 mm, Waters, Milford, MA) was used for chromatographic separation. A gradient with mobile phase A (0.1% formic acid) and mobile phase B (acetonitrile) was used at a flow rate of 0.3 mL/min with effluent split so that 20% was directed to the MS. B% changed as follows: 20% (0 min), 90% (1.6 min), 90% (3.0 min), 20% (3.7 min), and 20% (4.5 min). Detection was by positive ESI on TSQ quantum (ThermoFinnigan, San Jose, CA). The

multiple reaction monitoring (MRM) transition was m/z 517 to m/z 186 with collision energy of 22 eV for muraglitazar. The standard curve ranged from 0.05 to 5 µg/mL, and was fitted to the a 1/x weighted quadratic regression model ($Y = 0.0053 + 0.8923*X$, $R^2 = 0.9999$).

Data Analysis. For each radiochromatographic profile, the average CPM value of the first eight fractions (column void volume) was subtracted from the CPM value of each subsequent fraction. Radioactivity profiles were prepared by plotting the resulting net CPM values against time-after-injection. Radioactive peaks in the chromatographic profiles were reported as a percentage of the total radioactivity (CPM) recovered during the HPLC run. The amount of each metabolite was calculated based on its percent distribution and total amount of the parent compound used in the incubation. The amounts of metabolites were averaged from duplicate or triplicate incubations and HPLC analyses. The K_m and V_{max} values of each enzyme were estimated by fitting the average data to the Michaelis-Menten equation, using a nonlinear regression analysis in Sigmaplot (Equation 1) as recommended in Bjornsson *et al.* (2004), although the data showed imperfect fitting because of limited substrate concentrations used. The relative contribution of each CYP enzyme to a particular metabolic pathway was predicted using Equations 2 and 3.

$$Vi = V_{max}[S]/(K_m+[S]) \quad (1)$$

$$vi = AiVi \quad (2)$$

$$Fi = vi/\Sigma vi \quad (3)$$

$$F_{CYPi} = \Sigma vi\ /\Sigma(\Sigma vi) \quad (4)$$

In the above equations, Vi refers to the individual velocity for the formation of a metabolite by each CYP enzyme; V_{max} and K_m refer to kinetic parameters; S refers to substrate concentrations; *v*i refers to the velocity for each CYP enzyme per mg microsomal protein; Ai refers to the nominal specific content of individual CYP proteins in HLM as pmole CYP/mg microsomal protein. The content of each CYP was taken from literature values determined by immunoquantitation (Rodrigues 1999); Fi refers to the relative contribution of each CYP enzyme to a particular metabolic pathway. The substrate concentration used in the calculation was 1, 2.5, or 3.8 μM, near steady state C_{max} plasma concentrations observed after a clinically effective dose of 5, 10, or 20 mg of muraglitazar (data not shown). The relative contribution of each enzyme (F_{CYPi}) to overall oxidative metabolism was calculated using Equation 4.

Percent inhibition was calculated based on disappearance of the parent compound or formation of a metabolite. For disappearance of muraglitazar:

% Inhibition = (muraglitazar concentration in the presence of inhibitor - muraglitazar concentration in the absence of inhibitor) / (muraglitazar concentration in control - muraglitazar concentration in the absence of inhibitor).

For formation of a metabolite:

% Inhibition = (amount of the metabolite in the absence of inhibitor - amount of the metabolite in the presence of inhibitor)/(amount of the metabolite in the absence of inhibitor).

RESULTS

***In vitro* metabolite profiles of [^{14}C]muraglitazar.** Figure 2 shows the biotransformation profiles of [^{14}C]muraglitazar in HLM in the presence of NADPH or UDPGA or in human hepatocytes. M1, M10, M11, M14, and M15 were the major metabolites of [^{14}C]muraglitazar in the HLM incubations in the presence of NADPH. Multiple radioactive peaks eluted between 17-23 min on the HPLC system used in these experiments and they represented a significant amount of radioactivity in incubations of HLM in the presence of NADPH and in human hepatocytes. This region included the *O*-dealkylated metabolite M1. Since there was minimal amount of M1 found *in vivo* humans following oral administration of [^{14}C]muraglitazar (Zhang et al., 2006; Wang et al., 2006), M1 and other radioactive peaks eluting in this region were not further characterized. In the presence of UDPGA, M13 was formed as a single metabolite in the HLM incubation. M13 was identified as the acylglucuronide metabolite of muraglitazar based on HPLC and MS analysis comparison with previous studies (Wang et al., 2006). In the 3-h incubation with human hepatocytes, both oxidative metabolites and M13 were prominent metabolites, suggesting that both oxidative and conjugative pathways were active. M13 existed as multiple isomers due to acyl migration in this 3-h incubation. Table 1 shows LC/MS identification of the primary metabolites of muraglitazar in human liver microsomes and hepatocyte incubations. M10, M11, M13, M14, and M15 had the same HPLC retention time, molecular ions, and fragmentation patterns as the previously identified metabolites in humans (Zhang et al., 2006; Wang et al., 2006).

Metabolism of muraglitazar catalyzed by CYP enzymes. [^{14}C]Muraglitazar was incubated with human cDNA expressed CYP enzymes to determine the catalytic turnover

by oxidation. Table 2 shows the metabolite distribution in incubations of [^{14}C]muraglitazar with individual cDNA expressed CYP enzymes. Only enzymes CYP2C8, 2C9, 2C19, 2D6, and 3A4 generated significant amounts of metabolites; all other CYP enzymes barely metabolized muraglitazar and metabolites M10, M11, M14, and M15 were very minor metabolites (<0.5%) in these incubations. Figure 3 shows the biotransformation profiles of [^{14}C]muraglitazar in CYP2C8, 2C9, 2C19, 2D6, and 3A4. The parent drug was the largest radioactive peak in all incubations. M10 and M15 were major metabolites of CYP2C8. M10 was the major metabolite of CYP2C9. M10 and M11 were major products of CYP2C19. The significant metabolites of CYP2D6 were M10 and M15. M10, M14, and M15 were major metabolites of CYP3A4. CYP3A5 produced very small amounts of M10 and M15 but not M14 (data not shown). One radioactive peak eluted after the parent compound in some incubations was not characterized. M1 was formed in incubations of CYP3A4, 2D6, 2C8, and 2C9. Oxazole-ring opening metabolites M9 and M16 were observed in incubations of CYP2D6, 3A4, 2C9, and 2C8, suggesting that these enzymes might be involved in generation of M9 and M16. These results demonstrated that the major in vitro oxidative metabolites of muraglitazar are predominantly formed by CYP enzymes CYP2C8, 2C9, 2C19, 2D6, and 3A4 and not by CYP1A2, 2A6, 2B6, 2C18, 2E1, or 3A5.

Effects of enzyme inhibitors on oxidative metabolism of muraglitazar. Table 3 shows inhibition of muraglitazar metabolism results by anti-CYP antibodies and chemical inhibitors in human liver microsomes by monitoring the disappearance of muraglitazar at 2.5 μM. Anti-CYP1A2, 2A6, 2B6, 2E1 antibodies inhibited the disappearance of muraglitazar by <10%, and anti-CYP2C8, 2C9, 2Cs (2C8, 2C9, 2C18, and 2C19), 2D6,

and 3A4 significantly inhibited the disappearance of muraglitazar. Approximately 50% of muraglitazar clearance was inhibited by antibodies or chemical inhibitors of 2C enzymes and the another half was inhibited by antibodies or chemical inhibitors of CYP2D6 and 3A4. CYP2C8 antibody and montelukast inhibited muraglitazar clearance by >35% while the CYP2C19 antibody and benzylnirvanol did not seem to inhibit the disappearance of muraglitazar significantly.

Inhibition of muraglitazar disappearance by montelukast and anti-CYP2C8 antibody was mainly due to inhibition of formation of M15, a major metabolite of muraglitazar incubation in HLM B (Figure 4). This result is consistent with that from cDNA expressed enzymes showing that CYP2C8 was responsible for formation of M15. However, M15 was not as a significant metabolite in HLM A as in HLM B (Figures 2 and 4), which might explain the apparent larger contribution of CYP2C8 from the inhibition study in HLM B. The relatively less contribution of CYP2C9 and CYP2C19 from the inhibition study in HLM B than that obtained from the scaling of intrinsic clearance of muraglitazar (to be discussed) may be also due to the reduced concentrations of CYP2C9 and CYP2C19 in HLM B compared to HLM A. A reduced concentration of a CYP enzyme would reduce the rate of its metabolism (Vmax = kE, where E is the CYP concentration and k is an intrinsic reactivity constant), which will reduce the apparent inhibition effect by inhibitors when the disappearance of parent compound was monitored.

Inhibition effects of chemical inhibitors and the anti-CYP2C8 antibody on formation of oxidative metabolites M10, M11, M14, and M15 of muraglitazar were evaluated in HLM incubations, and the results are shown in Table 4 and Figure 4. 1-Aminobenzotriazole, a non-selective time-dependent CYP inhibitor, reduced the formation of all metabolites to

near background levels, suggesting that these metabolites were formed by CYP enzymes. Both the anti-CYP2C8 antibody and montelukast appeared to selectively inhibit M15 formation by >70%. Ketoconazole was a specific inhibitor to CYP3A4 at a low concentration (e.g. 1 μM), but also inhibited other enzymes such as CYP2C8, CYP2C9, CYP2C19, and CYP2D6 at higher concentrations (Ong et al., 2000; Stresser et al., 2004). Ketoconazole significantly inhibited formation of all metabolites at a concentration of 10 μM with a greater potency towards inhibition of M14 formation (>91%). Tranylcypromine reduced the formation of M11 to near background level. Sulfaphenazole inhibited formation of M10, M11, and M14 by 30-43%. Quinidine appeared to inhibit formation of M11 and M14. Selective inhibitors of CYP1A2 and 2B6, furafylline and ophenadrine, showed minor inhibition for formation of these metabolites; while the CYP2A6 inhibitor, 8-methoxypsoralen (Zhang et al., 2001), seemed to lead to a minor activation with formation of M10 and M15 metabolites.

Kinetic determination for muraglitazar oxidative metabolism. The enzyme kinetic parameters for the formation of the primary oxidative metabolites of muraglitazar by HLM and expressed CYP enzymes and the predicted relative contribution of each enzyme to metabolism of muraglitazar at different drug concentrations are shown in Table 5. The formation of M10, M11, M14, and M15 in HLM appeared to follow apparent Michaelis-Menten kinetics with Km values of 9-40 μM (Figure 5 and Table 5). In human liver microsomal incubations, M10 appeared to be formed by multiple enzymes since data points follow multiple trends; in contrast, M11, M14, and M15 appeared to be formed by individual enzymes. These results are consistent with those obtained from incubations with cDNA-expressed enzymes and with inhibitors in human liver

microsomes. Figure 6 shows the substrate concentration-dependent formation of metabolites M10, M11, M14, and M15 in the cDNA expressed enzymes. Based on the calculated intrinsic clearance (Cl_{int}) and relative contribution (Fi) values, CYP2C19 is predicted to be the major enzyme responsible for the 17-hydroxylation of muraglitazar (M11) and to contribute to 36% of muraglitazar total oxidative metabolism. CYP2C8 is predicted to be the major enzyme responsible for *O*-demethylation of muraglitazar (M15) and to contribute to 12% of muraglitazar total oxidative metabolism. CYP3A4 is predicted to be the major enzyme responsible for 9-hydroxylation of muraglitazar (M14) and to contribute up to 36% of muraglitazar total oxidative metabolism. CYP2C8, 2C9, 2C19, and 3A4 were involved in 12-hydroxylation of muraglitazar. Apparent K_m values for M14 and M15 formation were somewhat lower in HLM than in the expressed enzymes. Table 5 also shows that although initial metabolism rates Vi and scaled initial rates *V*i depend on the substrate concentrations with a given set of Ai (CYP content in HLM, pmol P450/mg microsomal proteins), relative contribution of each enzyme to formation of individual metabolite did not significantly change with the substrate concentrations. Based on the calculation (F_{CYPi}), the contribution of each enzyme to the overall oxidative metabolism of muraglitazar followed the order of CYP2C19 ≈ 3A4 > 2C8 ≈ 2C9 > 2D6 (Table 6).

Glucuronidation of muraglitazar. [^{14}C]Muraglitazar glucuronide was produced in incubations with HLM, UGT1A1, 1A3, and 1A9, but not with UGT1A6, 1A8, 1A10, 2B4, 2B7, and 2B15 (Figure 7). Figure 8 shows the concentration-dependent formation rate for [^{14}C]muraglitazar glucuronide in UGT1A1, 1A3, and 1A9. There appeared to be substrate inhibition of muraglitazar glucuronidation at substrate concentrations higher

than 30 μM (data not shown). The enzyme kinetic parameters of muraglitazar glucuronidation are shown in Table 7. The apparent K_m values of muraglitazar glucuronidation were similar among UGT1A1, 1A3, 1A9, and human liver microsomes (2.1 - 3.8 μM).

DISCUSSION

The common approaches for identifying the enzyme(s) responsible for metabolic pathways include: 1) incubations with commercially available human cDNA expressed enzymes to evaluate the metabolic turnover of a compound, 2) inhibition of the in vitro metabolism of the compound in human liver microsomes by enzyme specific inhibitors (antibodies or chemicals), and 3) correlation studies comparing the CYP or UGT activity towards metabolism of an unknown to a substrate known to be metabolized by a single enzyme in a panel of human liver microsome samples isolated from individual donors (Tang et al. 2005). However, whenever multiple enzymes are involved in the formation of one metabolite or one metabolic pathway, the inhibitor experiments can yield results that are difficult to interpret because of non-specific inhibition by chemical inhibitors, sub-maximal inhibition by chemical inhibitors or antibodies, and substrate concentration dependent inhibition. Correlation studies with a panel of human liver microsomes isolated from individual donors was also very difficult to interpret when multiple enzymes are involved in the metabolism of a given substrate. As early studies showed that multiple metabolic pathways were important for muraglitazar clearance, expressed enzymes were used as the primary technique to identify the enzymes for metabolism of muraglitazar. An evaluation of the metabolic turnover of muraglitazar with expressed enzymes was conducted to determine the CYP enzymes that demonstrated catalytic activity. Upon initial screening with cDNA expressed enzymes, multiple CYP (2C8, 2C9, 2C19, 2D6, and 3A4) and UGT (1A1, 1A3, and 1A9) enzymes were found to be involved in the oxidation and glucuronidation of muraglitazar. Furthermore, more than one enzyme was found to catalyze formation of several of the individual metabolites. Further

studies with selective chemical CYP inhibitors showed a complicated inhibition pattern, however, the inhibition of formation of the primary oxidative metabolites in HLM gave results in general agreement with the results found from the studies with the cDNA-expressed enzymes.

Since muraglitazar was oxidized by multiple CYP enzymes, the disappearance of the parent compound was monitored to evaluate the effects of inhibitors on overall metabolism of muraglitazar at a clinically efficacious concentration of 2.5 μM. The results showed that both chemical inhibitors and antibodies of CYP2C8, 2C9, 2D6, and 3A4 inhibited the clearance of muraglitazar in HLM. However, the inhibition study with anti-CYP2C19 antibody and benzylnirvanol, a CYP2C19 inhibitor, suggested that CYP2C19 did not significantly contribute to the clearance of muraglitazar in the microsomal incubations. From the study with cDNA expressed enzymes, CYP2C19 was the only enzyme responsible for formation of M11 and the formation of M11 was strongly inhibited by tranylcypromine, another CYP2C19 inhibitor. The formation of M11 was a significant clearance pathway for muraglitazar in humans (Zhang et al., 2006). The reason for this discrepancy is not clear, however, it may be due to: 1) the difficulty in measuring small changes in parent disappearance despite the non-linear reaction conditions employed leading to significant parent depletion (30-40%), and 2) the liver concentration of muraglitazar was not reflected by the plasma concentration and was actually higher than 2.5 μM.

The intrinsic clearance (V_{max}/K_m) values of individual CYPs were used to estimate the contributions of each CYP enzyme to the overall oxidative metabolism of muraglitazar and to formation of particular oxidative metabolites. The intrinsic clearance of each CYP

enzyme was determined through enzyme kinetic studies with cDNA expressed enzymes. When multiple enzymes are involved in the formation of one metabolite, Venkatakrishnan et al. (2001a and b) used the relative activity approach to scale from heterologously expressed enzymes to human liver microsomes. Additionally, Rodrigues (1999) has described a method to normalize reaction rates measured with individual expressed enzymes with respect to the nominal specific content of the corresponding CYP enzyme in the native human liver microsome samples. This method assumes that catalytic efficiency for a metabolic reaction in cDNA expressed enzyme is equivalent to that in HLM for the corresponding enzyme. Different sets of nominal specific enzyme contents for major CYP enzymes in the native human liver microsome samples estimated by immunoblotting have been published (Rodrigues, 1999; Venkatakrishnan et al., 2001a). The intrinsic clearance values determined in incubations with cDNA expressed enzymes and published values of the relative concentrations of each CYP enzyme expressed in an average human liver (Rodrigues, 1999) were used to estimate the contribution of each enzyme to the oxidative metabolism of muraglitazar. This estimation procedure does not consider the contribution of individual enzymes to formation of minor *in vivo* metabolites (M1, M9, M16) and a minor component that eluted after the parent in some incubations. M10 (12-hydroxylation) was predicted to be formed predominantly by CYP2C9 and 3A4. M11 (17-hydroxylation), M14 (9-hydroxylation), and M15 (*O*-demethylation) were predicted to be formed almost exclusively by CYP2C19, 3A4, and 2C8, respectively. Although the predicted contribution of each CYP enzyme to the overall clearance of muraglitazar, based on the scaling of intrinsic clearance, did not fully match the prediction from inhibition studies measuring the disappearance of the

parent compound, combined results from both approaches contributed to a better understanding of the clearance mechanisms of muragliatzar.

It is not possible to estimate the relative contribution of each of the three UGT enzymes demonstrated to form M13 in the expressed systems. This is due to the fact that the relative expression levels of different UGTs in expressed enzyme systems as well as in the human liver have not been determined. There is evidence that all three UGTs (UGT1A1, 1A3, and 1A9) that metabolize muraglitazar are expressed in the liver (Tukey and Strassburg, 2000). Highly expressed kidney UGT1A9 may also be involved in formation of M13, a significant urinary metabolite of muraglitazar. The lack of specific UGT inhibitors limits further estimation of the contribution of each UGT enzyme to the *in vivo* clearance of muraglitazar. Because of similar apparent K_m values for all three UGTs relative to the K_m value in HLM, their contributions to muraglitazar clearance are subject to their relative expression in tissues such as liver, gut, and kidney.

In summary, muraglitazar was demonstrated to be metabolized by multiple CYP-mediated oxidation and UGT-mediated conjugation pathways. These results suggested that the clearance of muraglitazar should not be dependent on a single enzyme in humans and therefore should not be dramatically affected by particular CYP or UGT inhibitors or inducers or by polymorphisms controlling the activity or expression of a single enzyme. Indeed, co-administration of muraglitazar with ketoconazole, an inhibitor of CYP3A4, and gemfibrozil, an inhibitor of CYP2C8, CYP2C9, CYP2C19, and UGT1A1 (Wen et al., 2001; Wang et al., 2002; Prueksaritanont et al., 2002; Oglivie et al., 2006) in human subjects did not produce substantial changes in muraglitazar exposure (data not shown), which further supports the overall conclusion drawn from these *in vitro* experiments.

Acknowledgements. We thank Dr. David Rodrigues for critical review of this work.

REFERENCES

Bjornsson TD, Callaghan JT, Einolf HJ, Fisher V, Gan L, Grimm S, Kao J, King P, Miwa G, Ni L, Kumar G, McLeod J, Obach RS, Roberts S, Roe A, Shah A, Snikeris F, Sullivan JT, Tweedie D, Vega JM, Walsh J, Wrighton SA (2003) The conduct of in vitro and in vivo drug-drug interaction studies: a pharmaceutical research and manufacturers of America (PhRMA) perspective. *Drug Metab Dispos* **31:** 815-832.

Devasthale PV, Chen S, Jeon Y, Qu F, Shao C, Wang W, Zhang H, Cap M, Farrelly D, Golla R, Grover G, Harrity T, Ma Z, Moore L, Ren J, Seethala R, Cheng L, Sleph P, Sun W, Tieman A, Wetterau JR, Doweyko A, Chandrasena G, Chang SY, Humphreys WG, Sasseville VG, Biller SA, Ryono DE, Selan F, Hariharan N, and Cheng PTW (2005) Design and synthesis of *N*-[(4-methoxyphenoxy)carbonyl] -*N*-[[4-[2-(5-methyl-2-phenyl-4-oxazolyl)ethoxy] phenyl]methyl]glycine, Muraglitazar /BMS-298585], a novel peroxisome proliferator-activated receptor α/γ dual agonist with efficacious glucose and lipid-lowering activities. *J Med Chem* **48:** 2248-2250.

Gelboin HV and Krausz K (2006) Monoclonal antibodies and multifunctional cytochrome P450 drug metabolism as paradigm. *J Clin Pharmacol* **46:** 353-372.

Harrity T, Farrelly D, Tienman A, Chu C, Kunselman L, Gu L, Cap M, Wu F, Shao C, Wang W, Zhang H, Fenderson W, Chen S, Devasthale P, Jeon Y, Seethala R, Yang WP, Ren J, Zhou M, Ryono D, Biller S, mookhtiar KA, Wetterau J, Gregg R, Cheng PT, and Harihara N (2006) Muraglitazar, a novel dual (alpha/gamma) peroxisome proliferator-activated receptor activator, improves diabetes and other metabolic abnormalities and preserves beta-cell function in db/db mice. *Diabetes* **55(1):** 240-248.

Huang YC, Colaizzi JL, Bierman RH, Woestenborghs R, Heykants J (1986) Pharmacokinetics and dose proportionality of ketoconazole in normal volunteers. *J Antimicrob Chemother* ***30:*** 206-210.

Kendall DM, Rubin CJ, Mohideen P, Ledeine LM, Beller R, Gross J, Norwood P, O'Mahony M, Sall K, Sloan GG, Roberts A, Fiedorrek FT, Defronzo RA (2006) Improvement of glycemic control, triglycerides, and HDL cholesterol levels with muraglitazar, a dual ([alpha]/[gamma]) peroxisome proliferator-activated receptor activator, in patients with type 2 diabetes inadequately controlled with metformin monotherapy: A double-blind, randomized, pioglitazone-comparative study, *Diabetes Care* **29(5):** 1016-1023.

King CD, Green MD, Rios GR, Coffman BL, Owens IS, et al. (1996) The glucuronidation of exogenous and endogenous compounds by stably expressed rat and human UDP-glucuronosyltransferase 1.1. *Arch Biochem Biophys* **332:** 92-100.

Mancy A, Dijols S, Poli S, Guengerich P and Mansuy D (1996) Interaction of sulfaphenazole derivatives with human liver cytochromes P450 2C: molecular origin of

the specific inhibitory effects of sulfaphenazole on CYP 2C9 and consequences for the substrate binding site topology of CYP 2C9. *Biochemistry* **35:** 16205-16212.

Miners JO and Mackenzie PI (1991) Drug glucuronidation in humans. *Pharmacol Ther* **51**: 347-369.

Nelson DR, Koymans L, Kamataki T, Stegeman JJ, Feyereisen R, Waxman DJ, Waterman MR, Gotoh O, Coon MJ, Estabrook RW, et al. (1996) P450 superfamily: Update on new sequences, gene mapping, accession numbers and nomenclature. *Pharmacogenetics* **6:** 1-42.

Newton DJ, Wang RW, and Lu AY (1995) Cytochrome P450 inhibitors. Evaluation of specificities in the in vitro metabolism of therapeutic agents by human liver microsomes. *Drug Meta Dispos* **23:** 154-158.

Ogilvie BW, Zhang D, Li W, Rodrigues AD, Gipson AE, Holsapple J, Toren P, and Parkinson A (2006) Glucuronidation converts gemfibrozil to a potent, metabolism-dependent inhibitor of CYP2C8: implications for drug-drug interactions. *Drug Metab Dispos* **34:**191-197.

Ong CE, Coulter S, Birkett DJ, Bhasker CR, and Miners JO (2000) The xenobiotic inhibitor profile of cytochrome P4502C8. *Br J Clin Pharmacol* **50:** 573–580.

Prueksaritanont T, Zhao JJ, Ma B, Roadcap BA, Tang C, Qiu Y, Liu L, Lin JH, Pearson G, and Baillie TA (2002) Mechanistic studies on metabolic interactions between gemfibrozil and statins. *J Pharmacol Exp Ther* **301:** 1042–1051.

Rodrigues AD (1999) Integrated cytochrome P450 reaction phenotyping: Attempting to bridge the gap between cDNA-expressed cytochromes P450 and native human liver microsomes. *Biochem Pharmacol* **57 (5):** 465-80.

Senafi SB, Clarke DJ, and Burchell B (1994) Investigation of the substrate specificity of a cloned expressed human bilirubin UDP-glucuronosyltransferase: UDP-sugar specificity and involvement in steroid and xenobiotic glucuronidation. *Biochem J* **303 (Pt 1)**:233-240.

Stresser DM, Broudy MI, Ho T, Cargill CE, Blanchard AP, Sharma R, Dandeneau AN, Goodwin JJ, Turner SD, Erve JCL, Patten CJ, Dehal SS, and Crespi CL (2004) Highly selective inhibition of human CYP3A4 in vitro by azamulin and evidence that inhibition is irreversible. *Drug Metab Dispos* **32:** 105-112.

Suzuki H, Kneller B, Haining RL, Trager WF and Rettie AE (2002) (+)-*N*-3-Benzylnirvanol and (-)-*N*-3-benzyl-phenobarbital: new potent and selective in vitro inhibitors of CYP2C19. *Drug Metab Dispos* **30:** 235-239.

Tang W, Wang RW, and Lu AYH (2005) Utility of recombinant cytochrome P450 enzymes. A drug metabolism perspective. *Curr Drug Metab* **6:** 503-517.

Tukey RH, and Strassburg CP (2000) Human UDP-glucuronosyltransferase: Metabolism, expression, and disease. *Annu Rev Pharmacol Toxicol* **40:** 581-616.

Venkatakrishnan K, von Moltke LL, and Greenblatt DJ (2001a) Human drug metabolism and the cytochromes P450: Application and relevance of in vitro models. *J Clin Pharmacol* **41:**1149-1179.

Venkatakrishnan K, von Moltke LV, and Greenblatt DJ (2001b) Application of the relative activity factor approach in scaling from heterologously expressed cytochromes P450 to human liver microsomes: studies on amitriptyline as a model substrate. *J Pharmacol Exp Ther* **297:** 326-337.

Wang L, Zhang D, Swaminathan A, Cheng PTW, Xue Y, Mosqueda-Garcia R, Everett DW, and Humphreys WG (2006) Glucuronidation as a major metabolic clearance pathway of [^{14}C]muraglitazar in humans: Different metabolic profiles in subjects with or without bile collection. *Drug Metab Dispos* **34:** 427-439.

Walsky RL, Obach RS, Gaman EA, Gleeson JR, and Proctor WR (2005) Selective inhibition of human cytochrome P4502C8 by montelukast. *Drug Metab Dispos* **33**:413-418.

Wang J-S, Neuvonen M, Wen X, Backman JT, and Neuvonen PJ (2002) Gemfibrozil inhibits CYP2C8-mediated cerivastatin metabolism in human liver microsomes. *Drug Metab Dispos* **30:** 1352–1356.

Wen X, Wang J-S, Backman JT, Kivistö KT, and Neuvonen PJ (2001) Gemfibrozil is a potent inhibitor of human cytochrome P450 2C9. *Drug Metab Dispos* **29:** 1359–1361.

Wells PG, Mackenzie PI, Chowdhury JR, Guillemette C, Gregory PA, Ishii Y, Hansen AJ, Kessler FK, Kim PM, Chowdhury NR, and Ritter JK (2004) Glucuronidation and the UDP-glucuronosyltransferases in health and disease subjects. *Drug Metab Dispos* **32**:281-290.

Zhang D, Zhang H, Aranibar N, Hanson R, Cheng PTW, Huang Y, Bonacorsi S, Swaminathan A, Everett DW, and Humphreys WG (2006) Structure elucidation of human oxidative metabolites of muraglitazar: use of microbial bioreactors in the biosynthesis of metabolite standards. *Drug Metab Dispos* **34:** 267-280.

Zhang, W, Kilicarsln T, Tyndale RF, and Sellers EM (2001) Evaluation of methoxsalen, tranylcypromine, and tryptamine as specific and selective CYP2A6 inhibitors in vitro. *Drug Metab Dispos* **26:** 897-902.

Legends for Figures

Figure 1 In vitro oxidative and conjugative pathways of muraglitazar.

Figure 2 Typical HPLC-radiochromatographic profiles of [^{14}C]muraglitazar in HLM A incubations in the presence NADPH for 30 min at 37°C and [muraglitazar] = 26.6 μM, or UDPGA for 30 min at 37°C and [muraglitazar] = 4 μM or in human hepatocyte incubations for 3 h at 37°C and [muraglitazar] = 25 μM.

Figure 3 HPLC-radiochromatographic profiles of the 30-min incubations of [^{14}C]muraglitazar (26.6 μM) with cDNA expressed CYP2C8, CYP2C9, CYP2C19, CYP2D6, and CYP3A4 in the presence of NADPH.

Figure 4 HPLC-radiochromatographic profiles of the 30-min incubations of [^{14}C]muraglitazar (25 μM) in HLM B in the presence of the antibody or montelukast, the chemical inhibitor of CYP2C8.

Figure 5 Muraglitazar concentration-dependent metabolite formation in HLM A incubations in the presence of NADPH (A) Michaelis-Menten plot (B) Eadie-Hofstee plot. The units are μM for K_m and pmole/min/mg protein for V_{max}.

Figure 6 Muraglitazar concentration-dependent metabolite formation in 30-min incubations with cDNA expressed CYP2C9, CYP2C19, CYP2C8, CYP2D6, and CYP3A4 in the presence of NADPH. Various concentrations of muraglitazar were incubated with 40 pmol/mL the CYP enzymes for 30 min at 37°C. The units are μM for K_m and pmol/min/pmole P450 for V_{max}.

Figure 7 Formation of [^{14}C]muraglitazar glucuronide in human cDNA expressed UGT enzymes and human liver microsomes (HLM A) in 30-min incubations of [^{14}C]muraglitazar (26.6 μM).

Figure 8 Muraglitazar concentration-dependent metabolite formation in 30-min incubations with cDNA-expressed UGT1A1, UGT1A3, and UGT1A9 in the presence of UDPGA. The incubations were for 30 min at 37°C. The units are μM for K_m and pmol/min/mg protein for V_{max}.

DMD Fast Forward. Published on October 24, 2006 as DOI: 10.1124/dmd.106.011932
This article has not been copyedited and formatted. The final version may differ from this version.

Table 1. The primary metabolites of [^{14}C]muraglitazar in human liver microsomes in the presence of NADPH and UDPGA and in human hepatocytes

Compounds	**$(M+H)^+$ [b]**	**MW change**	**Major fragment ion (m/z)**	**Biotransformation [a]**
M10	533	+16	290, 202	12-hydroxylation
M11	533	+16	308, 202	17-hydroxylation
M13	693	+176	517, 292	glucuronidation
M14	533	+16	290, 202	9-hydroxylation
M15	503	-14	292, 186	*O*-demethylation
muraglitazar	517	0	292, 186	Parent

[a] Identification of muraglitazar metabolites in humans has been reported previously (Zhang et al., 2006; Wang et al., 2006).

[b] The analysis was by positive ESI LC/MS.

DMD Fast Forward. Published on October 24, 2006 as DOI: 10.1124/dmd.106.011932
This article has not been copyedited and formatted. The final version may differ from this version.

Table 2. Mean relative distribution (%) of [^{14}C]muraglitazar metabolites produced by human cDNA expressed CYP enzymes

Expressed CYP450	**Mean relative distribution (%) (n = 2)** [a]					
	Parent	**M10**	**M11**	**M14**	**M15**	**Total** [b]
HLM No-NADPH	94.77	0.39	0.06	0.12	0.25	95.59
HLM	85.59	3.13	0.78	1.27	1.86	92.63
1A2	90.21	0.54	0.23	0.06	0.30	91.64
2A6	89.32	0.49	0.08	0.08	0.26	90.23
2B6	90.25	0.51	0.00	0.00	0.00	90.76
2C8	89.42	1.12	0.07	0.22	1.87	92.70
2C9	90.64	3.03	0.13	0.05	0.32	94.17
2C18	91.75	0.50	0.06	0.12	0.25	92.68
2C19	68.40	6.33	18.24	0.13	0.26	93.36
2D6	82.90	1.11	0.41	0.07	0.76	85.25 [c]
2E1	93.84	0.31	0.08	0.08	0.16	94.47
3A4	81.39	2.56	0.17	3.82	0.67	88.61[d]
3A5	92.35	0.57	0.09	0.33	0.41	93.75

[a] Metabolites were selected based on those predominant in vivo human metabolites (Zhang et al., 2006). The variability between two runs was less than 15%.

[b] Total was less than 100% because low level of degradation products eluted between 17-22 min on HPLC were observed in all incubations including no-NADPH control incubations.

[c] Less than 90% because M9, M16, and other radioactive peaks were prominent peaks in the incubations.

[d] Less than 90% because M1, M9, M16 and other radioactive peaks were significant peaks in the incubations.

DMD Fast Forward. Published on October 24, 2006 as DOI: 10.1124/dmd.106.011932
This article has not been copyedited and formatted. The final version may differ from this version.

Table 3. Inhibition of muraglitazar clearance in pooled human liver microsome B by monoclonal inhibitory antibodies and chemical inhibitors

CYP [a]	**% Mean Inhibition (n=3)** [b]	
	Inhibitory Antibodies [c]	**Chemical Inhibitors** [d]
	1X conc. (2-5 µL/mL)	1X conc.
CYP2C8	38.2	37.9
CYP2C9	14.7	21.7
CYP2C19	7.6	2.5
CYP2Cs	58.3	NA
CYP2D6	28.7	15.3
CYP3A4	30.1	41.2
All	NA[f]	98.1 [e]
Total % Inhibition	119.3 (117.1)[g]	118.5

[a] Disappearance of the parent compound was monitored by LC/MS analysis and % parent disappearance of muraglitazar was <40% for all incubations.
[b] % Inhibition = (muraglitazar concentration in the presence of inhibitor - muraglitazar concentration in the absence of inhibitor) / (muraglitazar concentration in control - muraglitazar concentration in the absence of inhibitor). Positive control incubations was in the presence of 1.2 mM NADPH and negative control incubations were done in the absence of NADPH. The variability beteween runs was less than 15%.
[c] Monoclonal antibodies against human enzymes in mice. The 1X concentrations were based on published results (Gelboin and Krausz, 2006). Inhibition with monoclonal antibodies for CYP1A2, 2A6, 2B6, and 2E1 at 1X concentrations was less than 10%.
[d] Chemical inhibitors were montelukast for CYP2C8, sulfaphenazole for CYP2C9, benzylnirvanol for CYP2C19, quinidine for CYP2D6, ketoconazole for CYP3A4, and 1-aminobenzotriazole for all CYP enzymes and the respective 1X concentrations used were 3, 10, 1, 1, 1, and 1000 µM. At 5 µM, benzylnirvanol, quinidine, and ketoconazole inhibited 21.4, 21.5, and 39.9% muraglitazar metabolism.
[e] 1-Aminobenzotriazole was used to inhibit all CYP enzymes.
[f] Not applicable.
[g] Total % inhibition was the sum of inhibition by antibodies or chemical inhibitors for CYP2C8, 2C9, 2C19, 2D6, and 3A4 and the % inhibition in the parenthesis was a sum of antibody inhibition for CYP2Cs, 2D6, and 3A4.

DMD Fast Forward. Published on October 24, 2006 as DOI: 10.1124/dmd.106.011932
This article has not been copyedited and formatted. The final version may differ from this version.

Table 4. Effects of chemical inhibitors and antibodies on metabolism of [^{14}C]muraglitazar in human liver microsomal incubations

Inhibitor (concentration)	**% Inhibition [a]**			
	M10	**M11**	**M14**	**M15**
Antibody (1X, CYP2C8) [b]	18.2	- [d]	-	75.9
Montelukast (3 μM, CYP2C8) [b]	17.0	-	-	78.5
Sulfaphenazole (20 μM, CYP2C9) [c]	29.4	42.9	33.3	-
Tranylcypromine (30 μM, CYP2C19) [c]	38.2	71.4	58.3	40.9
Quinidine (15 μM, CYP2D6) [c]	5.9	57.1	41.7	4.5
Ketoconazole (10 μM, CYP3A4) [c]	38.2	57.1	91.7	59.1
1- Aminobenzotriazole (1 mM, All CYP) [c]	70.6	71.4	91.8	86.4

[a] % Inhibition = (amount of the metabolite in the absence of inhibitor - amount of the metabolite in the presence of inhibitor)/(amount of the metabolite in the absence of inhibitor).

[b] Human liver microsome B was used and muraglitazar concentration was 25 μM.

[c] Human liver microsome A was used and muraglitazar concentration was 26.6 μM.

[d] No inhibition observed.

Table 5. Enzyme kinetic parameters for the formation of the primary oxidative metabolites of [^{14}C]muraglitazar by CYP2C8, CYP2C9, CYP2C19, CYP2D6, and CYP3A4 and the predicted relative contributions of each CYP enzyme to the metabolite formation at substrate concentrations of 1, 2.5, 3.8, and 25 μM [a]

Metab	Enzyme	K_m (μM)	V_{max} [b]	CL_{int} (V_{max}/K_m) [c]	Vi [d]				*vi* [e]				Estimated Relative contribution Fi (%)			
					1	2.5	3.8	25	1	2.5	3.8	25	1	2.5	3.8	25
M10	CYP2C8	199	1.2	0.006	0.006	0.015	0.023	0.137	0.394	0.98	1.48	8.79	9.8	9.8	9.96	10.9
	CYP2C9	56.8	1.0	0.017	0.017	0.041	0.061	0.293	1.59	3.89	5.80	28.2	39.5	39.2	39.0	35.0
	CYP2C19	53.8	1.9	0.036	0.035	0.086	0.128	0.613	0.669	1.63	2.43	11.6	16.6	16.5	16.3	14.5
	CYP3A4	330	4.2	0.013	0.013	0.032	0.048	0.295	1.37	3.41	5.18	31.9	34.0	34.4	34.8	39.6
	HLM	39.1	0.28	0.006	-[f]	-	-	-	-	-	-	-	-	-	-	-
M11	CYP2C19	23.3	4.2	0.179	0.172	0.41	0.59	2.16	3.27	7.70	11.2	41.1	100	100	100	100
	HLM	33.6	0.068	0.002	-	-	-	-	-	-	-	-	-	-	-	-
M14	CYP3A4	80.2	1.9	0.024	0.024	0.058	0.088	0.459	2.57	6.30	9.47	49.5	100	100	100	100
	HLM	13.8	0.074	0.012	-	-	-	-	-	-	-	-	-	-	-	-
M15	CYP2C8	42.3	0.6	0.015	0.015	0.035	0.052	0.234	0.932	2.25	3.34	15.0	94.0	93.8	93.6	91.2
	CYP2D6	559	3.4	0.006	0.006	0.015	0.023	0.145	0.06	0.15	0.23	1.45	6.0	6.3	6.4	8.8
	HLM	9.3	0.095	0.010	-	-	-	-	-	-	-	-	-	-	-	-

[a] Kinetic values were estimated by Michaelis-Menten analysis. Vi refers to the individual velocity for the formation of a metabolite by each CYP enzyme; *v*i refers to the velocity for each CYP enzyme per mg microsomal protein; Fi refers to the relative contribution of each CYP enzyme to a particular metabolic pathway. Human hepatic P450 concentrations used for scaling (Ai) were 64, 96, 19, 10, 108 pmol/mg microsomal proteins for CYP2C8, 2C9, 2C19, 2D6, and 3A4, respectively (Rodrigues, 1999).

[b] The unit for Vmax was pmol/mg protein/min for HLM and pmol/pmol CYP/min for expressed enzymes.

[c] The unit for clearance was μL/mg protein/min for HLM and μL/pmol CYP/min for expressed enzymes.

[d] The unit for Vi was pmol/pmol CYP/min.

[e] the unit for *v*i was pmol/mg microsomal protein/min.

[f] Not applicable.

Table 6. Predicted relative contributions of CYP2C8, 2C9, 2C19, 2D6, and 3A4 to the overall oxidative metabolism of [^{14}C]muraglitazar in the human liver at muraglitazar concentrations of 1, 2.5, 3.8, and 25 μM

Enzyme	**F_{CYPi} (%) (Total relative contribution)[a]**			
	1 μM	2.5 μM	3.8 μM	25 μM
CYP2C8	12.2	12.3	12.3	12.7
CYP2C9	14.7	14.8	14.8	15.0
CYP2C19	36.3	35.5	34.8	28.1
CYP2D6	0.55	0.57	0.60	0.77
CYP3A4	36.3	36.9	37.5	43.4
Total	100	100	100	100

[a] Based on the formation of M10, M11, M14, and M15, without consideration of formation of M1, M9, M16, and other minor radioactive peaks.

DMD Fast Forward. Published on October 24, 2006 as DOI: 10.1124/dmd.106.011932
This article has not been copyedited and formatted. The final version may differ from this version.

Table 7. Formation of [^{14}C]muraglitazar glucuronide in human cDNA expressed UGT enzymes and human liver microsomes (HLM A)

Metabolite	**Enzyme**	**K_m [a] (μM)**	**V_{max} [a] (pmol/min/mg protein)**
M13	UGT1A1	3.8	309.9
	UGT1A3	3.7	668.0
	UGT1A9	2.1	80.0
	HLM	3.6	583.5

[a] Kinetic values were estimated by Michaelis-Menten kinetic analysis.

Figure 1

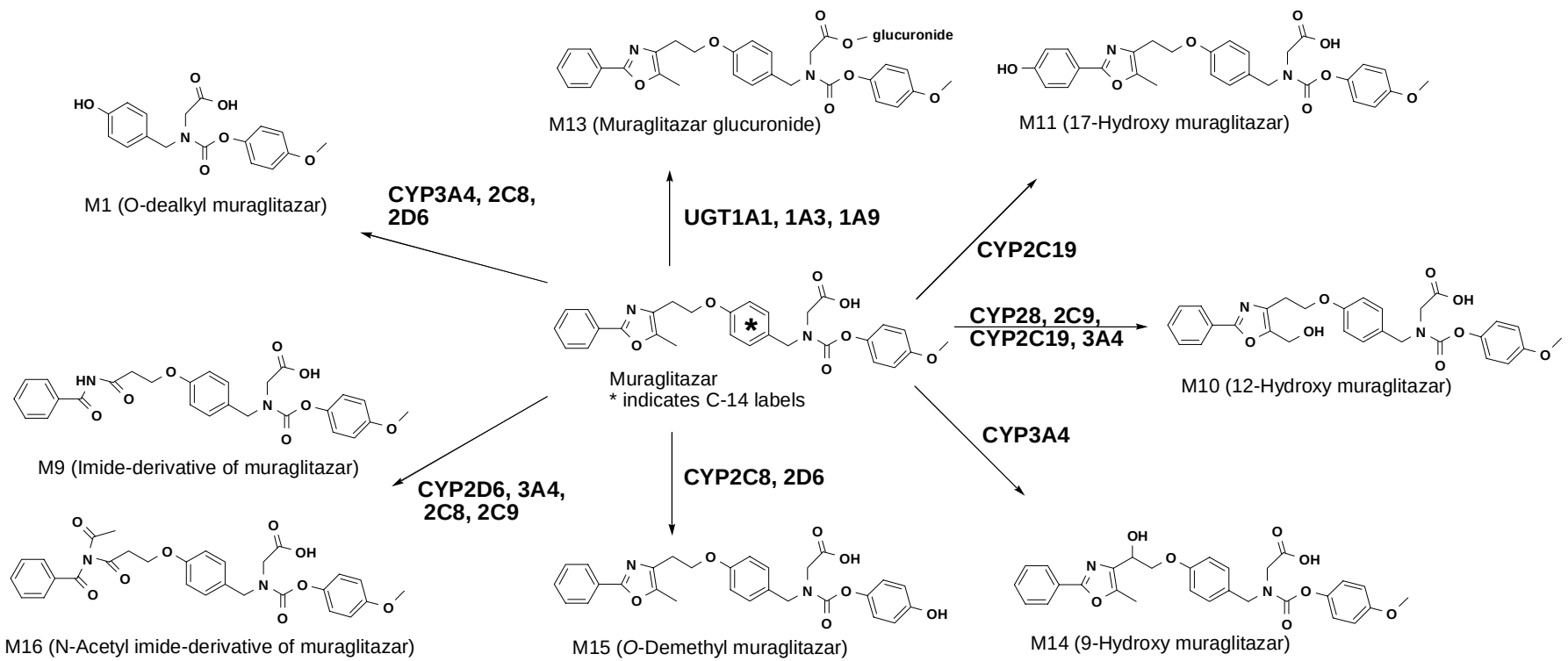

DMD Fast Forward. Published on October 24, 2006 as DOI: 10.1124/dmd.106.011932
This article has not been copyedited and formatted. The final version may differ from this version.

Figure 2

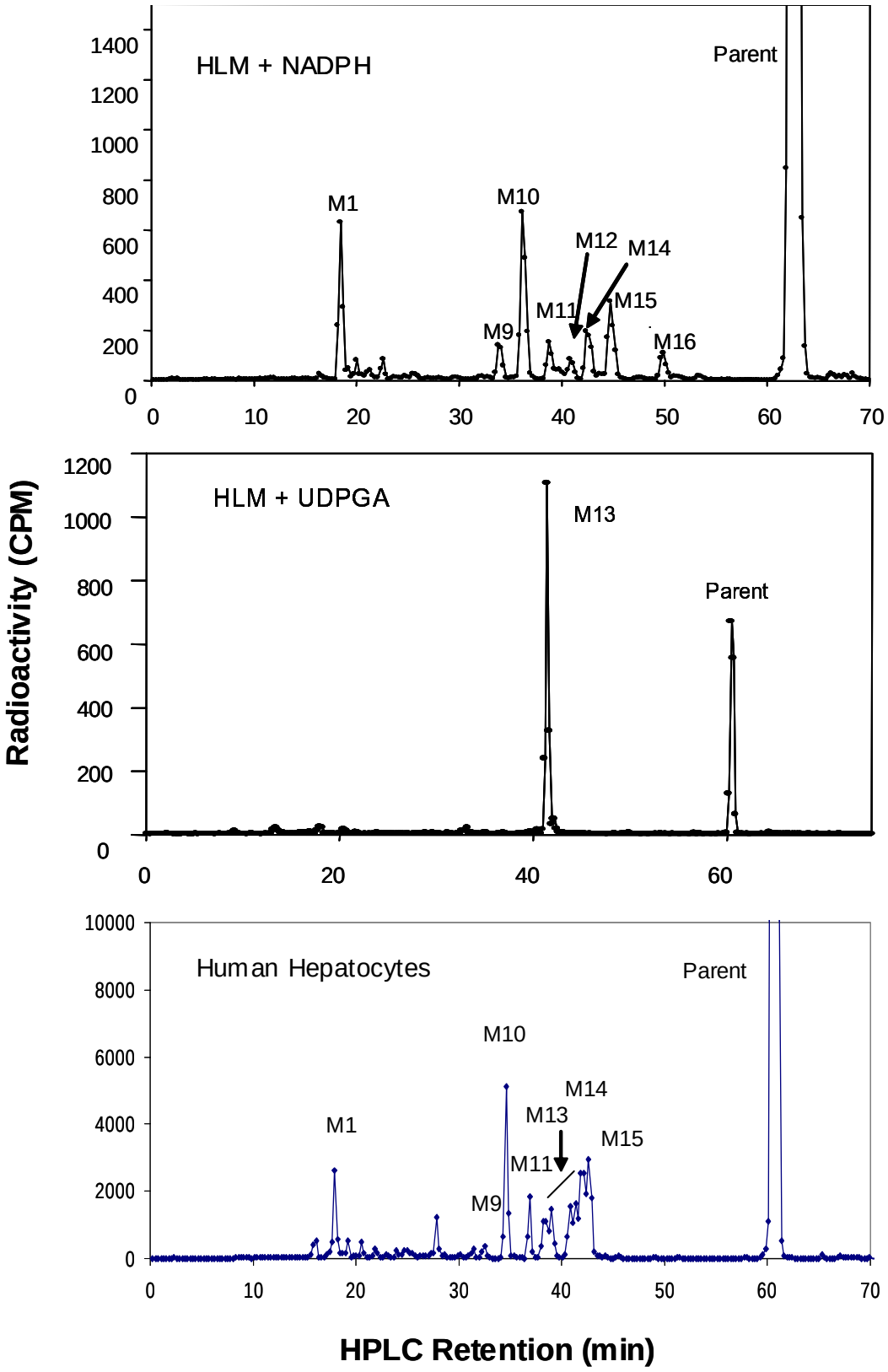

DMD Fast Forward. Published on October 24, 2006 as DOI: 10.1124/dmd.106.011932
This article has not been copyedited and formatted. The final version may differ from this version.

Figure 3

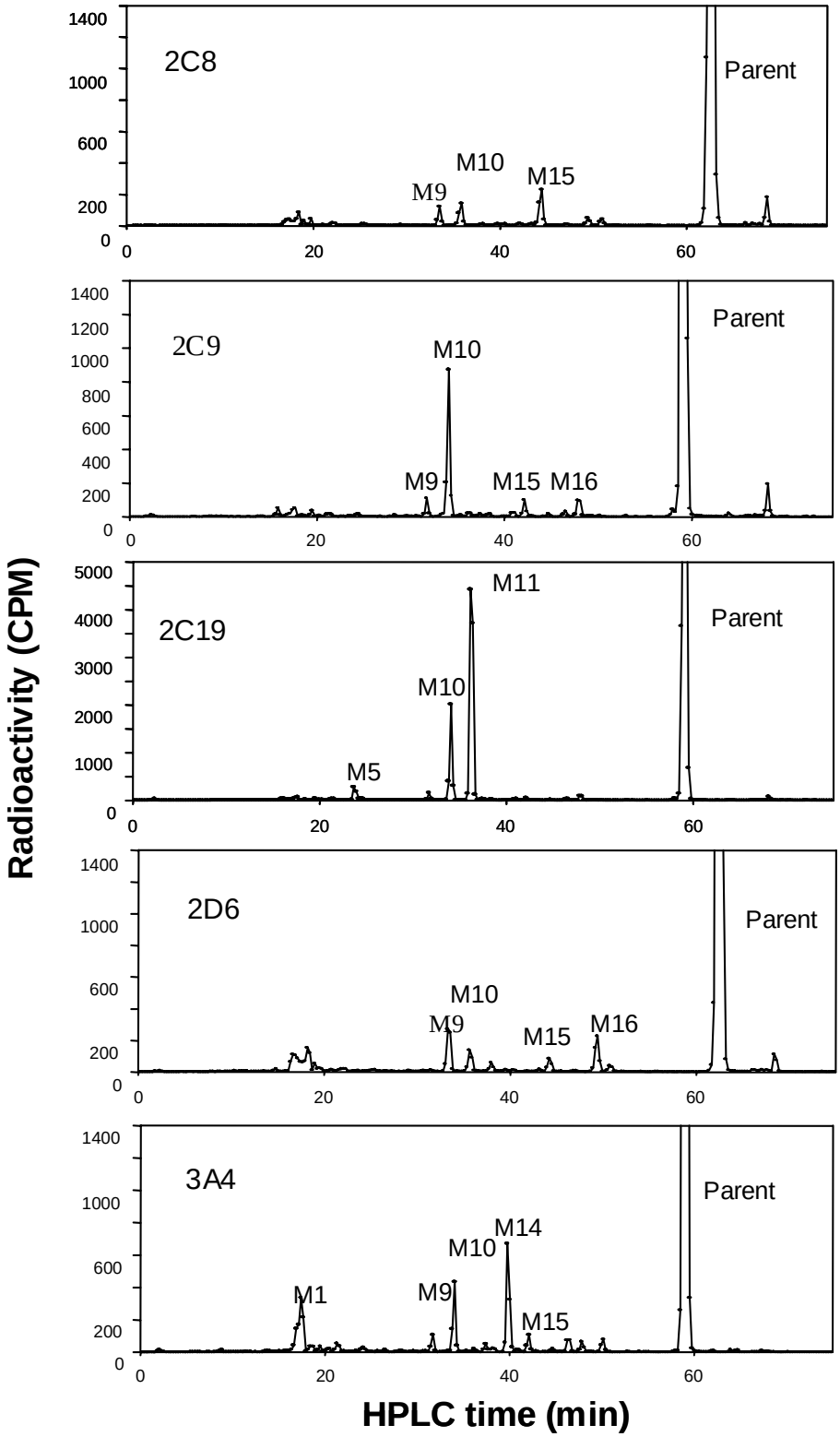

DMD Fast Forward. Published on October 24, 2006 as DOI: 10.1124/dmd.106.011932
This article has not been copyedited and formatted. The final version may differ from this version.

Figure 4

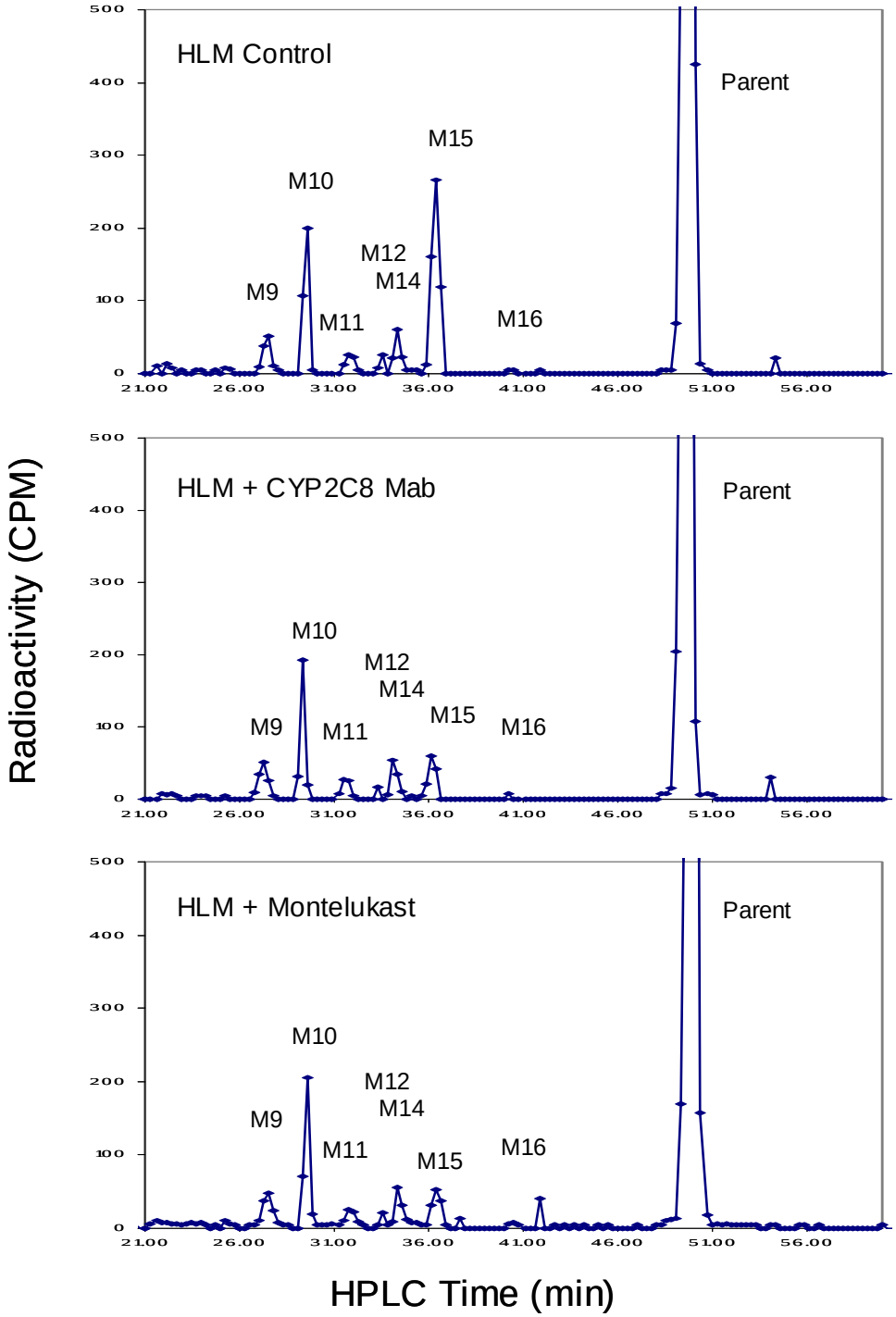

DMD Fast Forward. Published on October 24, 2006 as DOI: 10.1124/dmd.106.011932
This article has not been copyedited and formatted. The final version may differ from this version.

Figure 5

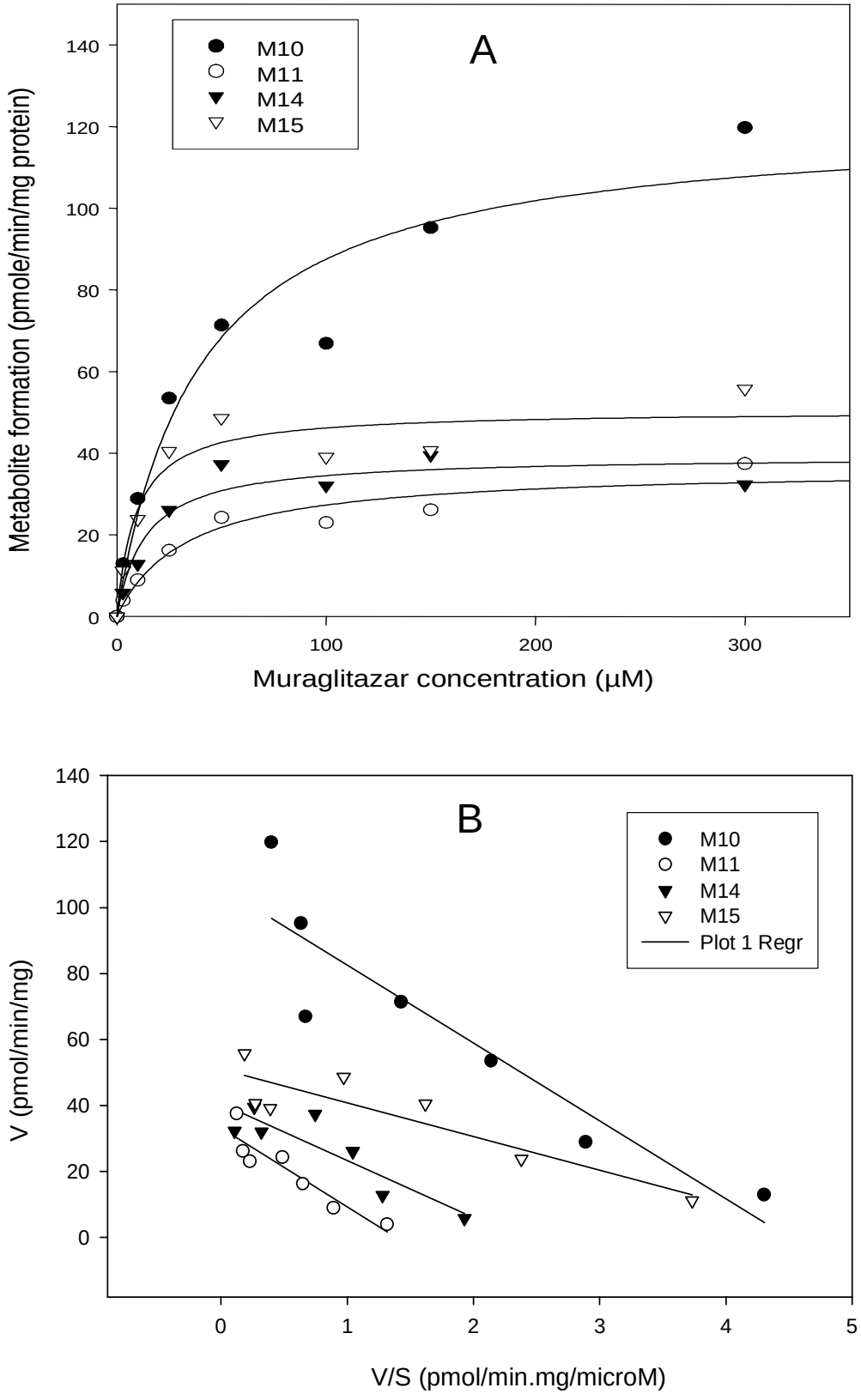

DMD Fast Forward. Published on October 24, 2006 as DOI: 10.1124/dmd.106.011932
This article has not been copyedited and formatted. The final version may differ from this version.

Figure 6

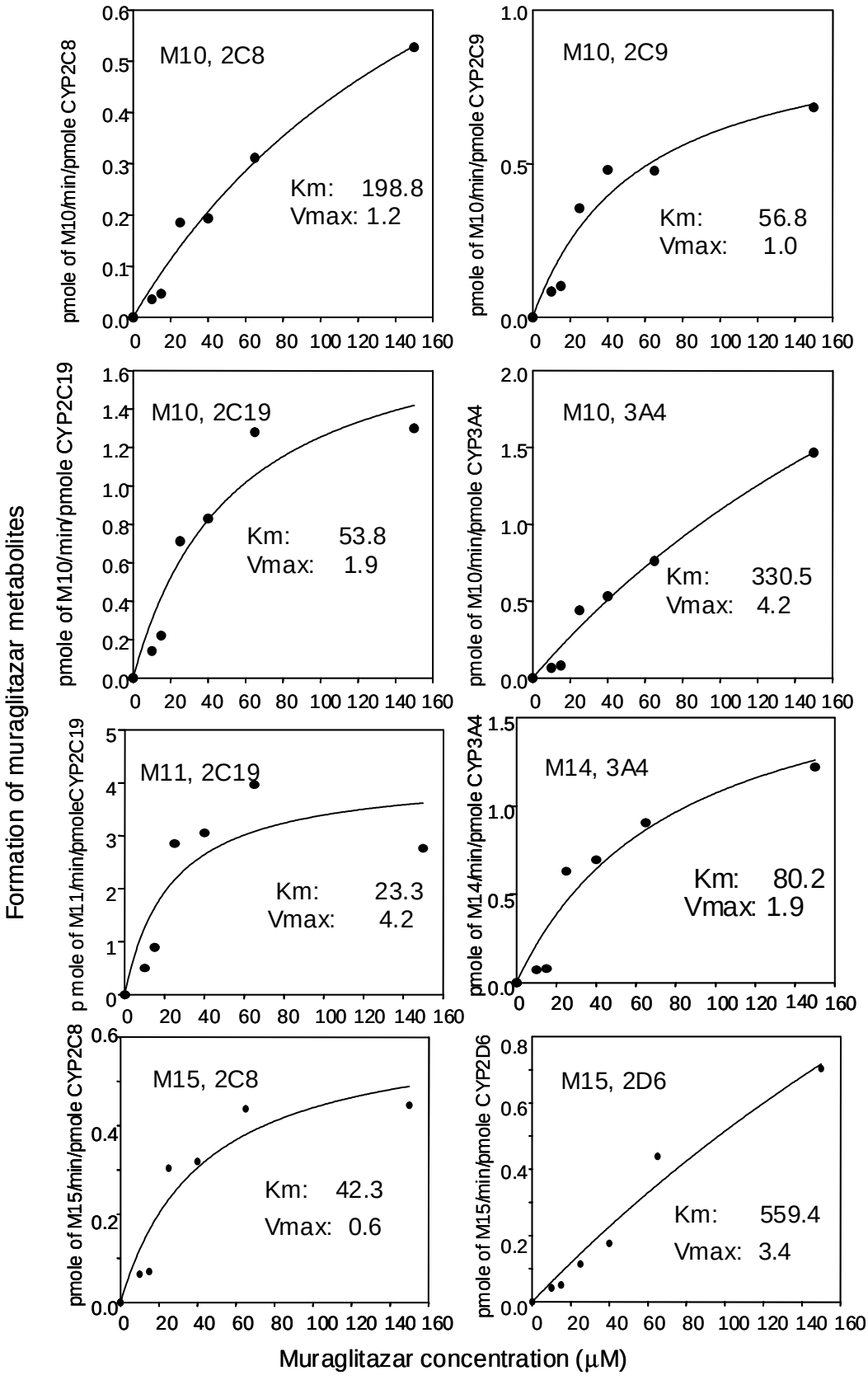

DMD Fast Forward. Published on October 24, 2006 as DOI: 10.1124/dmd.106.011932
This article has not been copyedited and formatted. The final version may differ from this version.

Figure 7

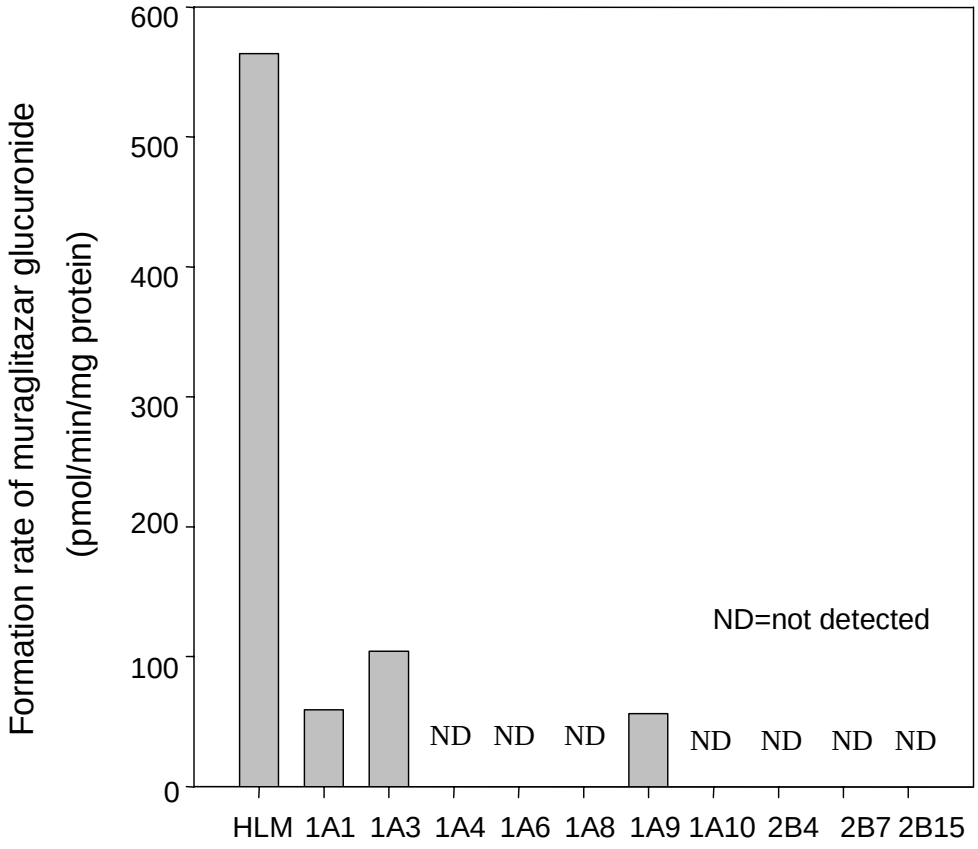

Data represent mean of a duplicate experiment and the variability was less than 15%.

DMD Fast Forward. Published on October 24, 2006 as DOI: 10.1124/dmd.106.011932
This article has not been copyedited and formatted. The final version may differ from this version.

Figure 8